Role of histamine H4 receptor ligands in bleomycin-induced pulmonary fibrosis

Role of Histamine H_4 Receptor ligands in Bleomycin-induced pulmonary fibrosis

Laura Lucarini[1*], Alessandro Pini[2*], Arianna Carolina Rosa[3], Cecilia Lanzi[1], Mariaconcetta Durante[1], Paul Louis Chazot[4], Stéphane Krief[5], Annemarie Schreeb[6], Holger Stark[7], Emanuela Masini[1]

Running title: Histamine H_4R ligands and pulmonary fibrosis

Departments of [1]NEUROFARBA, Section of Pharmacology, [2]Experimental and Clinical Medicine, Section of Histology, [3]Drug Science and Technology, University of Turin, Turin, Italy,[4] School of Biological & Biomedical Sciences, Durham University, Durham, UK; [5]Bioproject BIOTECH, Saint-Grégoire, France; [6]Institute of Pharmaceutical Chemistry, Johann-Wolfgang Goethe University, Frankfurt, and [7]Medicinal Chemistry, University of Dusseldorf, Dusseldorf, Germany.

* Laura Lucarini and Alessandro Pini contributed equally

Correspondence:

Emanuela Masini, MD

Department of NEUROFARBA, Section of Pharmacology

University of Florence

V.le G. Pieraccini n.6, 50139 Florence, Italy

Phone: +39 055 2758199

E-mail: emanuela.masini@unifi.it

ABSTRACT

Pulmonary fibrosis is a progressive and lethal disease characterized by inflammation and abnormal remodelling of lung parenchyma. The bleomycin model is the most accurate murine model in use. Bleomycin alters oxidant/antioxidant balance and activates pro-inflammatory cytokine production. The histamine H_4R plays an important role in the inflammatory process. The aim of this study was to investigate the role of different H_4R ligands in controlling inflammatory and fibrotic processes induced by bleomycin.

C57BL/6 mice were treated with vehicle, JNJ7777120 (JNJ, a selective H_4R antagonist) or ST-1006 (partial H_4R agonist), ST-994 (a H_4R neutral antagonist) and ST-1012 (an inverse H_4R agonist) at equimolar doses, released by micro-osmotic pumps for 21 days. Airway resistance to inflation was assayed and lung tissue processed to evaluate the production of oxidative stress markers, such as malondialdehyde (TBARS) and 8-hydroxy-2'-deoxyguanosine (8OH*d*G); inflammation markers, such as myeloperoxidase (MPO), COX_2 and PGE_2; fibrosis with TGF-β and tissue remodelling evaluating by percentage of positive Goblet cells and thickness of smooth-muscle layer.

Our results indicate that JNJ, ST-994 and ST-1012 exert an anti-inflammatory effect, as shown by the significant decrease of PGE_2, MPO, and TBARS. They also reduce Goblet cell hyperplasia, thickness of smooth-muscle layer, pro-fibrotic cytokine TGF-β levels and collagen deposition. These effects are accompanied by a decrease in airway resistance to inflation.

Our results indicated that H_4R blockade is associated with an anti-inflammatory and anti-fibrotic effect and may offer a new treatment strategy for the Th2-dependent lung inflammatory disease.

Keywords: Histamine H_4 receptors, Histamine H_4 ligands, Bleomycin, Inflammation, Lung fibrosis, TGF-β.

Abbreviations: COX-2, Cyclooxygenase-2; H_4R, Histamine H_4 receptor; 8OH*d*G, 8-hydroxy-2'-deoxyguanosine; JNJ7777120, 1-[(5-chloro-1H-indol-2yl)carbonyl]-4methylpiperazine; MPO, Myeloperoxidase; PGE_2, Prostaglandin E_2; ROS, Reactive oxygen species; TBARS**,** Thiobarbituric acid-reactive substances; TGFβ, transforming growth factor β; ST-994, N^4-(4-methylbenzyl)-6-(4-methylpiperazin-1-yl)pyrimidine-2,4-diamine;ST-1006,N^4-(2,6-dichlorobenzyl)-6-(methylpiperazin-1-yl)pyrimidine-2,4-diamine; ST-1012, N^4-(1,3-dihydro-2H-isoindol-2-yl)-6-(4-methylpiperazin-1-ylo)pyrimidine-2-amine.

1. Introduction

Pulmonary fibrosis is a pathological response of the lung to inflammation and chronic injury that manifests as abnormal and excessive deposition of collagen and other extracellular matrix components. Indeed, following epithelial cell injury, there is accumulation of vascular exudates and inflammatory cells within the injured alveolar space. The vascular exudates participate in the organization of extracellular tissue together with the influx and proliferation of fibroblasts and the emergence of the hallmark myofibroblast from resident cells and the transformation of epithelial cells or circulating fibrocytes. The myofibroblasts are activated fibroblasts organized into aggregation of cells known as fibroblastic *foci* and, ultimately, connective tissue matrix, especially collagen, accumulates and the fibrosis becomes established [1]. This process results in a progressive airway stiffening and thickening of the air-blood membrane, making breathing difficult and eventually leading to respiratory failure. Among the fibrotic diseases of the lung, idiopathic pulmonary fibrosis (IPF) is the most common disease with a prevalence that appeared to have increased by ~5% each year over the decade 1993–2002 [2,3] and with a high mortality rate and a median survival of ~3 years [4]. Actually, there is no effective therapy available which can favourably influence the course of the disease [5,6], the treatments are usually symptomatic and some patients require lung transplantation [5]. The use of anti-inflammatory agents, such as glucocorticoids, or immunosuppressive medications has been the conventional pharmacological approach, although current reviews suggest that there is no therapeutic benefit with these drugs in comparison with their significant side effects [7]. Therefore, novel treatment options, oriented towards novel substances and/or based on new therapeutic targets, which could override the efficacy and safety limitations of the existing anti-inflammatory drugs, are urgently required.

Oxidative stress is thought to play an important role in the pathogenesis of lung inflammation, increasing neutrophil sequestration in the pulmonary microvasculature and gene expression of proinflammatory mediators [8]. Moreover, several lines of evidence confirm the

association between mast cells and the development of fibrosis [9,10]. An increased number of mast cells was found in biopsy specimens from fibrotic lungs [11] and bleomycin-induced pulmonary fibrosis model [12]. Taken together, these findings suggest that mast cell-derived mediators could contribute to pulmonary fibrosis. In fact, it has been reported that mast cells play a crucial role in smooth muscle hypertrophy and in mucus hypersecretion, by releasing proteases such as tryptase, and growth factors [13]. Although the relationship between mast cells and fibrosis/tissue remodelling remains unclear, it has been reported that the histamine released by mast cells could contribute to the modulation of profibrotic stimuli, thus playing an important role in controlling fibrotic responses. Histamine is a pleiotropic mediator that exerts its biological effects through the interaction with four different G-protein-coupled receptor subtypes (H_1R-H_4R) [14]. In general, the H_1R plays an important role in allergic responses, the H_2R regulates gastric acid secretion, the H_3R, a presynaptic receptor, present mainly in the Central Nervous System, controls neurotransmitter release [15], and the H_4R, present in hematopoietic cells, activates mast cell, eosinophil and neutrophil migration [16,17]. Moreover, Kohyama and coworkers [18] demonstrated that the H_4R mediates *in vitro* the profibrotic effects of histamine on human foetal lung fibroblasts. In fact, the histamine effect on potentiating fibronectin-induced lung fibroblast migration was blocked by the selective H_4 antagonist JNJ7777120 (JNJ). These data suggest that the histamine H_4R could represent an attractive target for the development of new drugs for IPF treatment [18].

The aim of the present study was to evaluate whether histamine H_4R ligands could have a therapeutic effect in an *in vivo* mouse model of bleomycin-induced lung fibrosis [19,20]. To support the rationale for this approach, we investigated the effects of different H_4R ligand classes in controlling inflammation and fibrosis in an *in vivo* mouse model of bleomycin-induced pulmonary fibrosis.

2. Methods

2.1. Characterization of histamine H_4 receptor ligands in different screening models.

The affinity for histamine H_4 receptors (H_4R) was evaluated on ^{3}[H]-histamine displacement assay on membrane preparation from Chinese hamster ovary (CHO)-K1 cells which stably express the human H_4R and the efficacy was evaluated on functional binding assay using ^{35}[S] GTPyS on membrane preparation from stable CHO-hH_4R. Functional gene reporter assay was performed in CHO-dukx cells stably expressed both the mouse H_4R and luciferase gene under the control of MRE/CRE responsive elements [21] and stimulated by forskolin 0.3 μM. Reference full agonist for efficacy was imetit in the mouse H_4R gene reporter assay. pKi for histamine H_1 receptors (H_1R) was determined with ^{3}[H]-pyrilamine displacement assay on membrane preparation from CHO-K1 cells stably expressing the human H_4R [22] and on Sf9 cell membranes co-expressing *h*H1R and RGS4 [23]; pKi for histamine H_2 receptors (H_2R) was determined with ^{3}[H]-tiotidine displacement assay on Sf9 cell membranes with *h*H_2R-G$s\alpha_s$ fusion protein [23]; pKi for histamine H_3 receptors (H_3R) was performed with ^{3}[H]N^{α}-methylhistamine displacement on Sf9 cell membranes co-expressing *h*H_3R, Gα_{i2}, G$_{\beta 1\gamma 2}$ and RGS4 [23]. Ki(s) were calculated according to Cheng and Prusoff [24].

2.2. Animals

Male C57BL/6 mice, approximately 2 months old and weighing 25 to 30 g, were used for the experiments. They were purchased from a commercial source (Harlan, Udine, Italy), fed a standard diet, and housed for at least 48 h under a 12-h light/dark photoperiod before the experiments. The study protocol complied with the Declaration of Helsinki and the recommendations of the European Economic Community (86/609/CEE) on animal experimentation and was approved by the animal care committee of the University of Florence (Florence, Italy). Experiments were carried out at the Centre for Laboratory Animal Housing and Experimentation,

University of Florence. All studies involving animals are reported in accordance with the ARRIVE guidelines for reporting experiments involving animals [25,26].

2.3. Surgery and treatments

Fifty six mice were anesthetized with zolazepam/tiletamine (Zoletil, Virbac Srl, Milan, Italy; 50 μg/g i.p. in 100 μl of saline); 50 of them were treated with bleomycin (0.05 IU in 100 μl of saline), and the other six were treated with 100 μl of saline (referred to as non fibrotic negative controls, Saline), both delivered by intra-tracheal injection. Six mice were not underwent to surgery and used as control (Naïve).

The bleomycin treated mice, ten per group, were treated with continuous infusion of H_4R ligands by osmotic micropumps (Alzet, Cupertino, CA, USA) filled with 100 μl of PBS pH 7.4, containing the H_4R ligands at the reported concentrations: JNJ 7777120 40 mg/kg; ST 994 53 mg/kg; ST 1006 60 mg/kg; ST 1012 53 mg/kg (Table 1) Ten mice were treated only with PBS and referred to as fibrotic positive controls (Vehicle). The micropumps were implanted subcutaneously into a dorsal poach at day 0 and maintained for 21 days. They released 1,55 μl per day.

2.4. Functional assay of fibrosis

At day 21 after surgery, the mice were subjected to measurement of airway resistance to inflation, a functional parameter related to fibrosis-induced lung stiffness, by using a constant volume mechanical ventilation method [27,28]. In brief, upon anaesthesia, the mice were operated on to insert a 22-gauge cannula (Venflon 2; Viggo Spectramed, Windlesham, UK, 0.8 mm diameter) into the trachea and then ventilated with a small-animal respirator (Ugo Basile, Comerio, Italy), adjusted to deliver a tidal volume of 0.8 ml at a rate of 20 strokes/min. Changes in lung resistance to inflation, defined as pressure at the airway opening (PAO), were registered by a high-sensitivity pressure transducer (P75 type 379; Harvard Apparatus Inc., Holliston, MA) connected to a polygraph (Harvard Apparatus Inc. Edenbridge, UK; settings: gain 1, chart speed 25 mm/s).

Changes in lung resistance to inflation (as the pressure at the airway opening, PAO), measured for at least 3 min and expressed as millimetres, were carried out on at least 40 consecutive tracings of respiratory strokes and then averaged.

2.5. Lung tissue sampling

After the functional assay, the animals were killed with an overdose of anesthetic, and the whole left lungs were excised and fixed by immersion in 4% paraformaldehyde in phosphate-buffered saline for histological analysis. The right lungs were weighed, quickly frozen, and stored at −80°C. When needed for the biochemical assays, these samples were thawed at 4°C, homogenized on ice in 50 mM Tris-HCl buffer containing 180 mM KCl and 10 mM EDTA, pH 7.4, and then centrifuged at 10,000g, 4°C, for 30 min, unless otherwise reported. The supernatants and the pellets were collected and used for separate assays as detailed below.

2.6. Histology and assessment of collagen deposition, Goblet cell hyperplasia, and smooth muscle layer thickness

Histological sections, 6 μm thick, were cut from the paraffin-embedded lung samples. All sections were stained in a single session to minimize artifactual differences in the staining. Photomicrographs of the histological slides were randomly taken with a digital camera connected to a light microscope equipped with a x10 or x40 objective. Quantitative assessment of the stained sections was performed by computer-aided densitometry. Measurements of optical density (OD) and surface area were carried out using the free-share ImageJ 1.33 image analysis program (http://rsb.info.nih.gov/ij).

For assessment of lung collagen, the sections were stained with a simplified Azan method for collagen fibers according to Smolle *et al*., [29] with minor modifications, in which azocarminium and orange G were omitted to reduce parenchymal tissue background. OD measurements of the aniline blue-stained collagen fibers were carried out upon selection of an

appropriate threshold to exclude aerial air spaces and bronchial/alveolar epithelium, according to Formigli *et al*. [30]. Values are means ± SEM of the OD measurements (arbitrary units) of individual mouse (five images each) from the different experimental groups.

For morphometry of smooth muscle layer thickness and bronchial Goblet cell number, both key markers of airway remodelling, lung tissue sections were stained with hematoxylin and eosin or with periodic acid-Schiff (PAS) staining for mucins, respectively. Digital photomicrographs of medium- and small-sized bronchi were taken at random. Measurements of the thickness of the bronchial smooth muscle layer were carried out on the digitized images using the above-mentioned software. PAS-stained Goblet cells and total bronchial epithelial cells were counted on bronchial cross-section profiles, and the percentage of Goblet cells was calculated. For both parameters, values are means ± SEM of individual mouse (five images each) from the different experimental groups (tested blind).

2.7. Western blot analysis for H_4R and COX-2 protein expression

The total protein for the lung samples were obtained as described previously [31]. Lung tissues were lysed with buffer containing 0.9% NaCl, 20 mmol/L Tris-HCl (pH 7.6), 0.1% Triton X-100, 1 mmol/L phenylmethylsulfonyl fluoride, and 0.01% leupeptin, and homogenized. The total proteins (80 μg) as evaluated with the use of a bicinchoninic acid protein assay were subjected to Western blot and immunoblotting analysis as previously described [32]. The loading transfer of equal amounts of proteins were ascertained by either reblotting the membrane with an anti-tubulin antibody and/or staining the membrane with Ponceau S. The primary antibodies used were anti-H_4R polyclonal antibody (1,5 μg/mL, ab97997, Abcam, Cambridge, UK), anti-COX-2 polyclonal antibody (1:500, sc7951, Santa Cruz, Dallas, Texas, USA) and anti-β actin goat polyclonal antibody (1:500; ab8229, Abcam, Cambridge, UK). The binding of each primary antibody was determined by the addition of suitable peroxidase-conjugated secondary antibodies (anti-goat and anti-rabbit antibodies 1:15000). Densitometric analysis was performed with the ImageJ software.

2.8. Determination of myeloperoxidase (MPO)

This tissue indicator of leukocyte recruitment was determined in aliquots (100 µl) of lung homogenate supernatants, using a commercial ELISA kit (CardioMPO; Prognostix Inc., Cleveland, OH, USA), according to the manufacturer's instructions. The values are expressed as mU/mg of lung tissue (wet weight).

2.9. Determination of Prostaglandin E_2 (PGE_2)

The levels of PGE_2, the major cyclooxygenase product generated by activated inflammatory cells, were measured in aliquots (100 µl) of lung homogenate supernatants by using commercial ELISA kits (Cayman Chemical, Ann Arbor, MI), following the protocol provided by the manufacturer. The values are expressed as ng/mg of proteins, the latter determined with the Bradford method [32].

2.10. Determination of thiobarbituric acid-reactive substances (TBARS)

TBARS, such as malondialdehyde, are end-products of cell membrane lipid peroxidation by reactive oxygen species (ROS) and are considered reliable markers of oxidative tissue injury. They were determined by the measurement of the chromogen obtained from reaction of TBARS with 2-thiobarbituric acid [33]. In brief, 0.5 ml of 2-thiobarbituric acid (1% w/v) in 50 mM NaOH and 0.5 ml of HCl (25% w/v in water) were added to the lung tissue pellets. The mixture was placed in test tubes, sealed with screw caps, and heated in boiling water for 10 min. After cooling, the chromogen was extracted in 3 ml of 1-butanol, and the organic phase was separated by centrifugation at 2,000 *g* for 10 min. The absorbance of the organic phase was read spectrophotometrically at 532 nm wavelength over a standard curve of 1,1,3,3-tetramethoxypropane. The values are expressed as ng/mg of proteins, the latter determined as previously described [32].

2.11. Determination of 8-hydroxy-2'-deoxyguanosine (8OHdG)

Frozen lung samples were thawed at room temperature, and cell DNA isolation was performed as previously described [34] with minor modifications. The samples were homogenized in 1 ml of 10 mM PBS, pH 7.4, sonicated on ice for 1 min, added to 1 ml of 10 mM Tris-HCl buffer, pH 8, containing 10 mM EDTA, 10 mM NaCl, and 0.5% SDS, and incubated for 1 h at 37°C with 20 μg/ml RNase. Samples were incubated overnight at 37°C in the presence of 100 μg/ml proteinase K. Afterwards, the mixture was extracted with chloroform/isoamyl alcohol (10:2 v/v). DNA was precipitated from the aqueous phase with 0.2 volume of 10 M ammonium acetate, solubilized in 200 μl of 20 mM acetate buffer, pH 5.3, and denaturated at 90°C for 3 min. The extract was then supplemented with 10 IU of P1 nuclease in 10 μl and incubated for 1 h at 37°C with 5 IU of alkaline phosphatase in 0.4 M phosphate buffer, pH 8.8. All the procedures were performed in the dark. The mixture was filtered by an Amicon Micropure-EZ filter (Millipore Corporation, Billerica, MA), and 100 μl of each sample were used for 8OH*d*G determination by using an ELISA kit (JalCA, Shizuoka, Japan), following the instructions provided by the manufacturer. The values are expressed as ng/mg of proteins, the latter determined as previously reported [32].

2.12. Determination of Transforming Growth Factor-β (TGF-β)

The levels of TGF-β, the major profibrotic cytokine involved in fibroblast activation [35], were measured on aliquots (100 μl) of lung homogenate supernatants by using the Flow Cytomix assay (Bender Medsystems GmbH, Vienna, Austria), following the protocol provided by the manufacturer. In brief, suspensions of anti-TGF-β-coated beads were incubated with the samples and with a TGF-β standard curve, and then with biotin-conjugated secondary antibodies and streptavidin-phycoerythrin. Fluorescence was read with a cytofluorimeter (Epics XL; Beckman Coulter, Milan, Italy). Values are expressed as pg/μg of protein, determined as previously reported [32].

2.13. Statistical Analysis

For each assay, data were reported as mean values (± SEM) of individual average measures of the different animals per group. Significance of differences among the groups was assessed by one-way ANOVA followed by Newman-Keuls *post hoc* test for multiple comparisons, or, when only two groups had to be compared, by Student's *t* test for unpaired values. Calculations were made with Prism 4.03 statistical software (GraphPad Software, Inc., San Diego, CA,USA).

3. Results

3.1. Functional assay of fibrosis

Intra-tracheal bleomycin caused a statistically significant increase in airway stiffness, as showed by the clear-cut elevation in the pressure at airway opening (PAO) in the fibrotic positive controls given vehicle (14.67 ± 0.08 mm) compared with the non-fibrotic negative controls (12.43 ± 0.40 mm). Both compounds JNJ and ST-994, two selective antagonists of histamine H_4R, and ST-1012, an inverse agonist, caused a statistically significant reduction of airway stiffness (13.16 ± 0.38, 13.11 ± 0.42 mm and 12.5 ± 0.49, respectively). The results of the functional assay are reported in Figure 1. No effects were shown with ST-1006, a partial agonist (14,36 ± 0,37) (Fig. 1).

3.2. Expression of histamine H_4 receptor in lung tissue

The administration of bleomycin caused a statistically significant increase in the H_4R protein expression in lung homogenates. The increased expression of H_4R protein was significantly reduced in lung samples obtained from JNJ-treated animals. All the other studied ligands determined a decrease in H_4R protein expression although did not reach statistical significance (Fig. 2, panel A and B).

3.3. Effects of H_4 Receptor ligands on inflammation and oxidative stress markers

Intra-tracheal bleomycin injection was found to cause lung inflammation. The extent of inflammatory infiltrate in the lung, mainly macrophages and neutrophils, was significantly increased in positive control animals after bleomycin administration as shown by the increase in MPO activity (Fig. 3). The treatment of the animals with all the selected H_4R ligands caused a statistically significant reduction of MPO activity.

To gain further insight into the effects of the different H_4R ligands on inflammation, COX-2 expression and activity were evaluated. As expected, all the H_4R ligands studied reduced bleomycin-induced COX-2 expression (Fig. 4, panel A). This effect resulted also in a significant

reduction of PGE_2 production, the major COX-2 product generated by activated inflammatory cells (Fig. 4, panel B). The production of MDA was evaluated as TBARS (Fig. 5, panel A), end-products of cell membrane lipid peroxidation by ROS and reliable markers of oxidative tissue injury. The production of TBARS was markedly increased in the fibrotic positive control compared with non-fibrotic negative one. As shown in Fig. 5, panel A, only the antagonists JNJ and ST-994 and the inverse agonist ST-1012 significantly reduced TBARS production.

Determination of 8OH*d*G (Fig. 5 panel B), an indicator of oxidative DNA damage, showed a similar trend as TBARS, markedly increased in the fibrotic positive control compared with the non-fibrotic one. The administration of JNJ, ST-994 and ST-1012 significantly reduced 8OH*d*G production. ST-1006 treatment did not affect TBARS and 8OH*d*G level.

3.4. Effects of H_4R ligands on fibrosis

The assay of TGF-β (Fig. 6), a major pro-fibrotic cytokine, showed that this molecule significantly increased in the bleomycin-treated animals as compared with the controls. Administration of all the selected histamine H_4R ligands caused a statistically significant reduction of TGF-β production. Morphological observation and computer-aided densitometry on Azan-stained sections (Fig. 7, panels A and B respectively), which allows the determination of the optical density (OD) of collagen fibers, revealed a significant increase in collagen deposition in the lungs of the bleomycin-treated animals compared with the non-fibrotic negative controls. The treatment with JNJ, ST-994 and ST-1012 caused a robust, near complete, reduction of the amount of lung collagen fibers (Fig. 7, panel B). No effects were shown with ST-1006.

Bronchial remodeling was evaluated by measuring the relative number of PAS-positive Goblet cells (Fig. 8, panel A) and thickness of the smooth muscle layer (Fig. 8, panel B), key histological parameters of inflammation-induced adverse bronchial remodeling [36]. As expected, both these parameters were significantly increased in the bleomycin-administered mice. Notably, all the tested compounds were able to significantly reduce the percentage of PAS-positive Goblet cells

versus total bronchial epithelial cells (Fig. 8, panel A), as well as the thickness of the airway smooth muscle layer (Fig. 8, panel B).

4. Discussion

This study offers evidence that histamine H_4R ligands could have therapeutic activity in a model of chemically induced lung fibrosis in the mouse. In our experiments, the H_4R ligands were administered in preventive mode, following the onset of bleomycin-induced lung injury.

Compounds JNJ, ST-994, and ST-1012 displayed robust anti-inflammatory and anti-fibrotic properties: in fact they consistently decreased the inflammatory and oxidative stress indicators, i.e. the number of infiltrating leukocytes evaluated as lung tissue MPO, COX-2 expression, PGE_2 levels, TBARS and 8OH*d*G production.

They also reduced Goblet cells hyperplasia, the thickness of smooth layer, the level of pro-fibrotic cytokine (TGF-β) and collagen deposition; all these parameters were accompanied by a decrease in airway resistance to inflation (PAO). Using a similar animal model of lung fibrosis, naproxen and NO-donating naproxen (CINOD), two classic anti-inflammatory drugs, were previously shown to inhibit lung inflammation and consequent fibrosis [28].

Chronic inflammatory conditions in the lung lead to permanent structural changes and remodeling of the airway walls of which fibrosis is a major constituent; in fact the treatment with bleomycin activates the inflammatory cascade, as clearly underlined by the increase in MPO activity, histamine H_4R and COX-2 protein expression (Fig. 2, 3 and 4), indicating an increase in the number of inflammatory cells migrated to the lung parenchyma. Histamine has been implicated in the pathophysiology of several inflammatory and immunological mechanisms, acting as a mediator of both acute and chronic phases. The function of histamine in cellular immunity, through the control of cytokine and chemokine production and migration of inflammatory cells, beyond its traditional role in mediating immediate airway hyper-responsiveness, has been defined [37].

Histamine H_4R antagonists have been demonstrated to exert anti-inflammatory activity in zymosan-induced peritonitis model in mice [38,39]. In this model, intra-peritoneal treatment of mice with zymosan induces neutrophil migration, which is blocked by an H_4R antagonist [40].

Accumulating experimental evidence indicates the role of H_4R in modulating allergic lung inflammation, mainly through its effects on Th2 cell induction [41].

In a model of dermal inflammation, the levels of several pro-inflammatory cytokines and chemokines, including IL_4, were increased in ear tissue on fluorescein isothiocyanate (FITC) challenge and inhibited by H_4R antagonist treatment [42]; in the same model, JNJ administration reduces the ear edema and the scratching response in a dose-dependent manner [43]. In a rat model of carrageenan-induced acute inflammation, H_4R antagonists reduced the early phase development of edema [28], and attenuated the hyperalgesic response to thermal stimuli, acting possibly through the peripheral nociceptive pathway [44]. Histamine H_4R are functionally expressed in cells of innate immune system [45] which includes NK cells, dendritic cells (DCs) and monocytes, although the expression of this receptor in monocytes is still controversial. Zhu *et al*.,[46] demonstrated a very low expression of H_4R in resting $CD14^+$ cells, others only in activated monocytes [47] or in THP-1 clone 15 cells, which highly secret TNFα and IL-1β, which in turn might induce the expression of H_4R [45]. The presence of protein expression of H_4R in cells of the innate immunity could explain how these cells localize at inflammation sites and the anti-inflammatory activity of H_4R antagonists. Indeed histamine is a robust chemotactic factor for these cells [45].

Our results highlighted that all the investigated H_4R ligands inhibit the production of TGF-β, a pro-fibrotic cytokine, and a recent identified target for the development of novel anti-fibrotic agents. In fact, drugs targeting the TGF-β pathway, such as anti-TGF-β monoclonal antibodies and the fibroblast inhibitor pirfenidone, hold great promise and were subject to clinical development [48]; however, although the preliminary data were encouraging, their therapeutic efficacy on patients with lung fibrosis still remains to be clearly demonstrated [49]. On the other hand, the strategy of targeting prostaglandin synthesis by COX inhibitors is questioned by controversial findings. Although they prevent and/or reduce lung collagen accumulation, inflammation and oxidative stress in bleomycin-induced lung fibrosis models [28], patients with pulmonary fibrosis have decreased PGE_2 levels and may benefit from PGE_2 administration [50]. There is thus still an

unmet need for selective, potent, and safe anti-fibrotic drugs. The results of the present study point to H_4R antagonists as novel, potential therapeutic agents with anti-inflammatory and anti-fibrotic activities, when administered in the inflammatory phase of the fibrotic onset. The debatable point that also molecules with agonistic activity have, in our experimental setting, some beneficial effect may be due to the fact that the histamine H_4R has high intrinsic activity in absence of the physiological agonist.

In conclusion, the dual effect of H_4R antagonists on inflammation and fibrosis point to their therapeutic potential for the treatment of Th2-mediated diseases, including pulmonary fibrosis.

Acknowledgements

This research was supported by a grant from Ente Cassa di Risparmio di Firenze (E. Masini). The authors are grateful to Isabelle Nagmarand and Aurélien Boudeau from Bioproject for their skillful technical assistance.

Conflict of interest

The authors declare that they have no conflicts of interest to disclose.

5. **References**

[1] R.M. du Bois, Strategies for treating idiopathic pulmonary fibrosis, Nat. Rev. Drug Discov. 9 (2010) 129-140.

[2] A.T. Society, American Thoracic Society. Idiopathic pulmonary fibrosis: diagnosis and treatment. International consensus statement. American Thoracic Society (ATS), and the European Respiratory Society (ERS), Am. J. Respir. Crit. Care Med. 161 (2000) 646-664.

[3] A.L. Olson, J.J. Swigris, D.C. Lezotte, J.M. Norris, C.G. Wilson, Brown KK, Mortality from pulmonary fibrosis increased in the United States from 1992 to 2003, Am. J. Respir. Crit. Care Med. 176 (2007) 277-284.

[4] S.K. Frankel, M.I. Schwarz, Update in idiopathic pulmonary fibrosis, Curr. Opin. Pulm. Med. 15 (2009) 463-9.

[5] H.P. Hauber, M. Blaukovitsch, Current and future treatment options in idiopathic pulmonary fibrosis, Inflamm. Allergy Drug Targets 9 (2010) 158-172.

[6] G. Raghu, H.R. Collard, J.J. Egan, F.J. Martinez, J. Behr, K.K. Brown, T.V. Colby, J.F. Cordier, K.R. Flaherty, J.A. Lasky, D.A. Lynch, J.H. Ryu, J.J. Swigris, A.U. Wells, J. Ancochea, D. Bouros, C. Carvalho, U. Costabel, M. Ebina, D.M. Hansell, T. Johkoh, D.S. Kim, T.E. Jr. King, Y. Kondoh, J. Myers, N.L. Muller, A.G. Nicholson, L. Richeldi, M. Selman, R.F. Dudden, B.S. Griss, S.L. Protzko, H.J. Schunemann, An official ATS/ERS/JRS/ALAT statement: idiopathic pulmonary fibrosis: evidence-based guidelines for diagnosis and management, Am. J. Respir. Crit. Care Med. 183 (2011) 788-824.

[7] N.J. Carter, Pirfenidone: in idiopathic pulmonary fibrosis, Drugs. 71(2011) 1721-1732.

[8] S. Cuzzocrea, M. Mazzon, L. Dugo, I. Serraino, A. Ciccolo, T. Centorrino, A.De Sarro, A.P. Caputi, Protective effects of n-acetylcysteine on lung injury and red blood cell modification induced by carrageenan in the rat, The FASEB J. 15 (2001) 1187-1200.

[9] F. Levi-Schaffer, E. Rubinchik, Mast cell role in fibrotic diseases, Isr. J. Med. Sci. 31 (1995) 450-453.

[10] S.R. Holdsworth, S.A .Summers, Role of mast cells in progressive renal diseases, J. Am. Soc. Nephrol. 19 (2008) 2254-2261.

[11] M. Sasaki, M. Kashima, T. Ito, A. Watanabe, M. Sano, M. Kagaya, T. Shioya, M. Miura, Effect of heparin and related glycosaminoglycan on PDGF-induced lung fibroblast proliferation, chemotactic response and matrix metalloproteinases activity, Mediators Inflamm. 9 (2000) 85-91.

[12] K. Zhang, M. Gharaee-Kermani, B. McGarry, D. Remick, S.H. Phan, TNF-alpha-mediated lung cytokine networking and eosinophil recruitment in pulmonary fibrosis, J. Immunol. 158 (1997) 954-959.

[13] A.J. Wardlaw, S. Dunnette, G.J. Gleich, J.V. Collins, A.B. Kay, Eosinophils and mast cells in bronchoalveolar lavage in subjects with mild asthma. Relationship to bronchial hyperreactivity, Am. Rev. Respir. Dis. 137 (1988) 62-69.

[14] T. Nguyen, D.A. Shapiro, S.R. George, V. Setola, D.K. Lee, R. Cheng, L. Rauser, S.P. Lee, K.R. Lynch, B.L. Roth, B.F. O'Dowd, Discovery of a novel member of the histamine receptor family, Mol. Pharmacol. 59 (2001) 427-433.

[15] P. Panula, P.L. Chazot, M. Cowart, R. Gutzmer, R. Leurs, W.L. Liu, H. Stark, R.L. Thurmond, H.L. Haas, International Union of Basic and Clinical Pharmacology. XCVIII. Histamine Receptors, Pharmacol. Rev. 67 (2015) 601-655.

[16] C.L. Hofstra, P.J. Desai, R.L. Thurmond, W.P. Fung-Leung, Histamine H4 receptor mediates chemotaxis and calcium mobilization of mast cells, J. Pharmacol. Exp. Ther. 305 (2003)1212-1221.

[17] K.F. Buckland, T.J. Williams, D.M. Conroy, Histamine induces cytoskeletal changes in human eosinophils via the H(4) receptor, Br. J. Pharmacol. 140 (2003) 1117-1127.

[18] T. Kohyama, Y. Yamauchi, H. Takizawa, S. Kamitani, S. Kawasaki, T. Nagase, Histamine stimulates human lung fibroblast migration, Mol. Cell. Biochem. 337 (2010) 77-81.

[19] N. Kaminski, J.D. Allard, J.F. Pittet, F. Zuo, M.J. Griffiths, D. Morris, X. Huang, D. Sheppard, R.A. Heller, Global analysis of gene expression in pulmonary fibrosis reveals distinct programs regulating lung inflammation and fibrosis, Proc. Natl. Acad. Sci. U S A. 97(2000) 1778-1783.

[20] A. Moeller, K. Ask, D. Warburton, J. Gauldie, M. Kolb, The bleomycin animal model: a useful tool to investigate treatment options for idiopathic pulmonary fibrosis?, Int. J. Biochem. Cell. Biol. 40 (2008) 362-382.

[21] L.R. Fitzgerald, I.J. Mannan, G.M. Dytko, H.L. Wu, P. Nambi, Measurement of responses from Gi-, Gs-, or Gq-coupled receptors by a multiple response element/cAMP response element-directed reporter assay, Ana.l Biochem. 275 (1999) 54-61.

[22] M. Tomasch, J.S. Schwed, L. Weizel, H. Stark, Novel chalcone-based fluorescent human histamine H3 receptor ligands as pharmacological tools, Front. Syst. Neurosci. 6 (2012) 14. doi: 10.3389/fnsys.2012.00014.

[23] K. Sander, K. Kottke, Y. Tanrikulu, E. Proschak, L. Weizel, E.H. Schneider, R. Seifert, G. Schneider, H. Stark, 2,4-Diaminopyrimidines as histamine H4 receptor ligands-Scaffold optimization and pharmacological characterization, Bioorg. Med. Chem., 17 (2009) 7186-7196

[24] Y. Cheng, W.H. Prusoff, Relationship between the inhibition constant (K1) and the concentration of inhibitor which causes 50 per cent inhibition (I50) of an enzymatic reaction, Biochem. Pharmacol. 22 (1973) 3099-3108.

[25] C. Kilkenny, W. Browne, I.C. Cuthill, M. Emerson, D.G. Altman, NC3Rs Reporting Guidelines Working Group, Br. J. Pharmacol. 160 (2010) 1577-1579.

[26] J. McGrath, G. Drummond, E. McLachlan, C. Kilkenny, C. Wainwright, Guidelines for reporting experiments involving animals:the ARRIVE guidelines, Br. J. Pharmacol. 160 (2010) 1573-1576.

[27] A. Pini, R. Shemesh, C.S. Samuel, R.A. Bathgate, A. Zauberman, C. Hermesh, A. Wool, D. Bani, G. Rotman, Prevention of bleomycin-induced pulmonary fibrosis by a novel antifibrotic peptide with relaxin-like activity, J. Pharmacol. Exp. Ther. 335 (2010) 589-99.

[28] A. Pini, S. Viappiani, M. Bolla, E. Masini, D. Bani, Prevention of bleomycin-induced lung fibrosis in mice by a novel approach of parallel inhibition of cyclooxygenase and nitric-oxide donation using NCX 466, a prototype cyclooxygenase inhibitor and nitric-oxide donor, J. Pharmacol. Exp. Ther. 341 (2012) 493-499.

[29] J. Smolle, M. Fiebiger, R. Hofmann-Wellenhof, H. Kerl, Quantitative morphology of collagen fibers in cutaneous malignant melanoma and melanocytic nevus, Am. J. Dermatopathol. 18 (1996) 358–363.

[30] L. Formigli, A.M. Perna, E. Meacci, L. Cinci, M. Margheri, S. Nistri, A. Tani, J. Silvertown, G. Orlandini, C. Porciani, Paracrine effects of transplanted myoblasts and relaxin on post-infarction heart remodelling, J. Cell. Mol. Med. 11 (2007) 1087–1110.

[31] F. Cianchi, C. Cortesini, L. Magnelli, E. Fanti, L. Papucci, N. Schiavone, L. Messerini, A. Vannacci, S. Capaccioli, F. Perna, M. Lulli, V. Fabbroni, G. Perigli, P. Bechi, E. Masini, Inhibition of 5-lipoxygenase by MK886 augments the antitumor activity of celecoxib in human colon cancer cells, Mol. Cancer. Ther. 5 (2006) 2716-2726.

[32] F. Cianchi, C. Cortesini, O. Fantappiè, L. Messerini, I. Sardi, N. Lasagna, F. Perna, V. Fabbroni, A. Di Felice, G. Perigli, R. Mazzanti, E. Masini, Cyclooxygenase-2 activation mediates the proangiogenic effect of nitric oxide in colorectal cancer, Clin. Cancer. Res. 10 (2004) 2694-2704.

[33] O.I. Aruoma, B. Halliwell, M.J. Laughton, G.J. Quinlan, J.M. Gutteridge, The mechanism of initiation of lipid peroxidation: evidence against a requirement for an iron (II)-iron (III) complex, Biochem. J. 258 (1989) 617–620.

[34] M. Lodovici, C. Casalini, R. Cariaggi, L. Michelucci, P. Dolara, Levels of 8-hydroxydeoxyguanosine as a marker of DNA damage in human leukocytes, Free. Radic. Biol. Med. 28 (2000) 13–17.

[35] T.A. Wynn, Cellular and molecular mechanisms of fibrosis, J. Pathol. 214 (2008) 199–210.

[36] T.R. Bai, D.A. Knight, Structural changes in the airways in asthma: observations and consequences, Clin. Sci. (Lond). 108 (2005) 463-77.

[37] P.J. Barnes, K.F. Chung, C.P. Page, Inflammatory mediators of asthma: an update, Parmacol. Rev. 50 (1998) 515-596.

[38] K. Takeshita, K. Sakai, K.B. Bacon, F. Gantner, Critical role of histamine H4 receptor in leukotriene B4 production and mast cell dependant neutrophil recruitment induced by zymosan in vivo, J. Pharmacol. Exp. Ther. 307 (2003) 1072-1078.

[39] R.L. Thurmond, P.J. Desai, P.J. Dunford, W.P. Fung-Leung, C.L. Hofstra, W. Jiang, A potent and selective histamine H4 receptor antagonist with anti-inflammatory properties, J. Pharmacol. Exp. Ther. 309 (2004) 404-413.

[40] R.L. Thurmond, E.W. Gelfand, P.J. Dunford, The role of histamine H1 and H4 receptors in allergic inflammation: the search for new antihistamines, Nat. Rev. Drug Discov. 7 (2008) 41-53.

[41] E. Zampeli, E. Tiligada, The role of histamine H4 receptor in immune and inflammatory disorders, Br. J. Pharmacol. 157 (2009) 24-33.

[42] S.A. Boehme, K. Franz-Bacon, E.P. Chen, et al, A small molecule CRTH2 antagonist inhibits FITC-induced allergic cutaneous inflammation, Int. Immunol. 21 (2009) 81-93.

[43] J.M. Cowden, M. Zhang, P.J. Dunford, R.L. Thurmond, The histamine H4 receptor mediates inflammation and pruritus in Th-2-dependant dermal inflammation, J. Invest. Derm. 130 (2010) 1023-1033.

[44] G. Coruzzi, M. Adami, E. Guaita, I.J. de Esch, R. Leurs, Anti-inflammatory and antinociceptive effects of the selective histamine H4-receptor antagonists JNJ7777120 and VUF6002 in a rat model of carrageenan-induced acute inflammation, Eur. J. Pharmacol. 563 (2007) 240-244.

[45] B.B. Damaj, C.B. Becerra, H.J. Esber, et al, Functional expression of H4 histamine receptor in human natural killer cells, monocytes, and dendritic cells, J. Immunol. 179 (2007) 7907-7915.

[46] Y. Zhu, D. Michalovich, H. Wu, K.B. Tan, G.M. Dytko, I.J. Mannan, R. Boyce, J. Alston, L.A. Tierney, X. Li, N.C. Herrity, L. Vawter, H.M. Sarau, R.S. Ames, C.M. Davenport, J.P. Hieble, S. Wilson, D.J. Bergsma, L.R. Fitzgerald, Cloning, expression and pharmacological characterization of a novel human histamine receptor, Mol. Pharmacol. 59 (2001) 434-441.

[47] R.H. Morse, R. Séguin, E.L. McCrea, J.P. Antel, Nk cell-mediated lysis of autologous human oligodendrocytes, J. Neuroimmunol. 116 (2001) 107-115.

[48] G.J. Prud'homme, Pathobiology of transforming growth factor β in cancer, fibrosis and immunologic disease, and therapeutic considerations, Lab. Invest. 87 (2007) 1077-1091.

[49] Z. Paz, Y. Shoenfeld, Antifibrosis: to reverse the irreversible, Clin. Rev. Allergy Immunol. 38 (2010) 276-286.

[50] Z. Borok, A. Gillissen, R. Buhl, R.F. Hoyt, R.C. Hubbard, T. Ozaki, S.I. Rennard, R.G. Crystal, Augmentation of functional prostaglandin E levels on the respiratory epitelial surface by aerosol administration of prostaglandin E, Ann. Rev. Resp. Dis. 144 (1991) 1080-1084.

Legends

Fig. 1
Spirometric evaluation. Bar graph and statistical analysis of PAO values (means ± SEM.) among the different experimental groups. Significance of differences (one-way ANOVA and Newman–Keuls post hoc test): *p < *0.05* *vs* Bleomycin + Vehicle.

Fig. 2
Western blot analysis of H_4R expression in the lung specimens from the different experimental groups (Panel A). The densitometric analysis of the bands was normalized to β-actin (Panel B). Data are representative of at least three independent experiments. Significance of differences (one-way ANOVA and Newman–Keuls post hoc test): **p<0.01 *vs* Bleomycin + Vehicle.

Fig. 3
Evaluation of leukocyte infiltration. Bar graph shows MPO levels in the lung tissue (means ± SEM) of the different experimental groups. Significance of differences (one-way ANOVA and Newman–Keuls post hoc test): **p<0.01 and ***p<0.001 *vs* Bleomycin + Vehicle.

Fig. 4
Western blot analysis of COX-2 expression in the lung specimens from the different experimental groups (Panel A). The densitometric analysis of the bands was normalized to β-actin (Panel B). Data are representative of at least three independent experiments. Prostaglandin production: bar graph shows the lung tissue levels of PGE_2 (means ± SEM) of the different experimental groups (Panel C). Significance of differences (one-way ANOVA and Newman–Keuls post hoc test): *p<0.05, **p<0.01 and ***p<0.001 *vs* bleomycin + vehicle.

Fig. 5
Evaluation of oxidative stress parameters. Bar graphs shows the lung tissue levels of TBARS (Panel A) and 8OH*d*G (Panel B) of the different experimental groups (means ± SEM). Significance of differences (one-way ANOVA and Newman–Keuls post hoc test): *p<0.05, **p<0.01 and ***p<0.001 *vs* Bleomycin + Vehicle.

Fig. 6
Evaluation of TGF-β. Bar graph shows the lung tissue levels of the profibrotic cytokine (means ± SEM) of the different experimental groups. Significance of differences (one-way ANOVA and Newman–Keuls post hoc test): ***p<0.001 *vs* Bleomycin + Vehicle.

Fig. 7
Evaluation of lung fibrosis. Representative micrographs of Azan-stained lung tissue sections from mice of the different experimental groups. Collagen fibers are deep blue stained. The lung from a fibrotic positive control shows marked fibrosis, which is absent in the lung from a non-fibrotic negative control and reduced by all the treatments. Scale bars, 50 μm. Densitometric analysis of Azan-stained sections is shown in bar graph as arbitrary OD units (means ± SEM). Significance of differences (one-way ANOVA and Newman–Keuls post hoc test): ***p<0.001 *vs* Bleomycin + Vehicle.

Fig. 8
Evaluation of Goblet cell hyperplasia (Panel A) and bronchial smooth muscle layer thickness (Panel B), shown as both the representative micrographs of the stained section and the relative densitometric analyses. The Goblet cells hyperplasia was measured by PAS staining and computer-aided morphometry in lung specimens of the different experimental group. The PAS-positive cells

are indicated by arrows. The histograms show the percentage of PAS-positive Goblet cells over total epithelial cells (means ± SEM) (Panel A). The smooth muscle thickness was assessed by computer-aided morphometry on hematoxylin and eosin-stained lung sections in lung specimens of the different experimental groups and indicated by double arrows. The histograms show the thickness of the smooth muscle (means ± SEM) (Panel B). Significance of differences (one-way ANOVA and Newman–Keuls post hoc test): *$p<0.05$ and **$p<0.01$ *vs* Bleomycin + Vehicle. Scale bar, 50 μm.

Fig. 1

Click here to download high resolution image

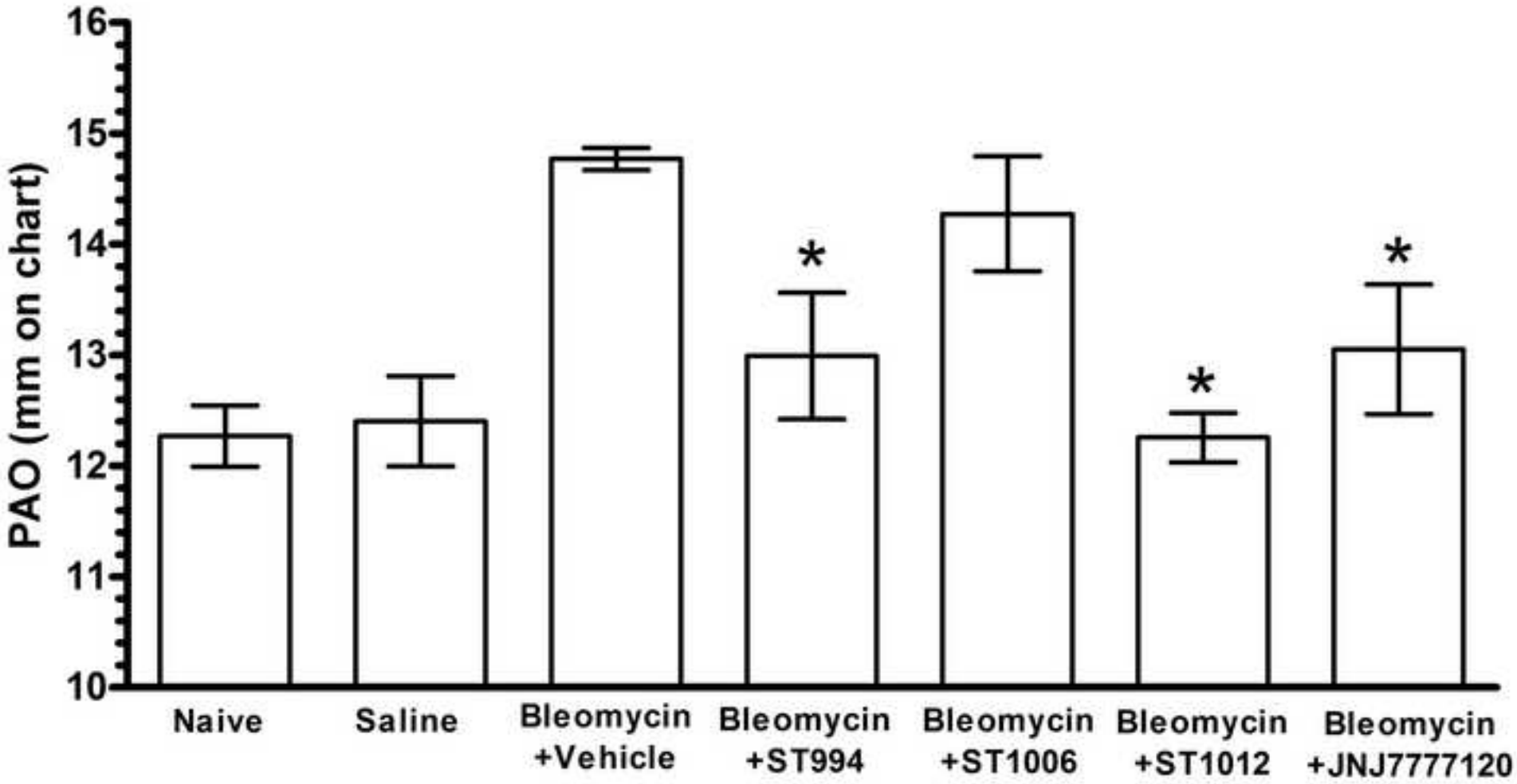

Fig. 2

Click here to download high resolution image

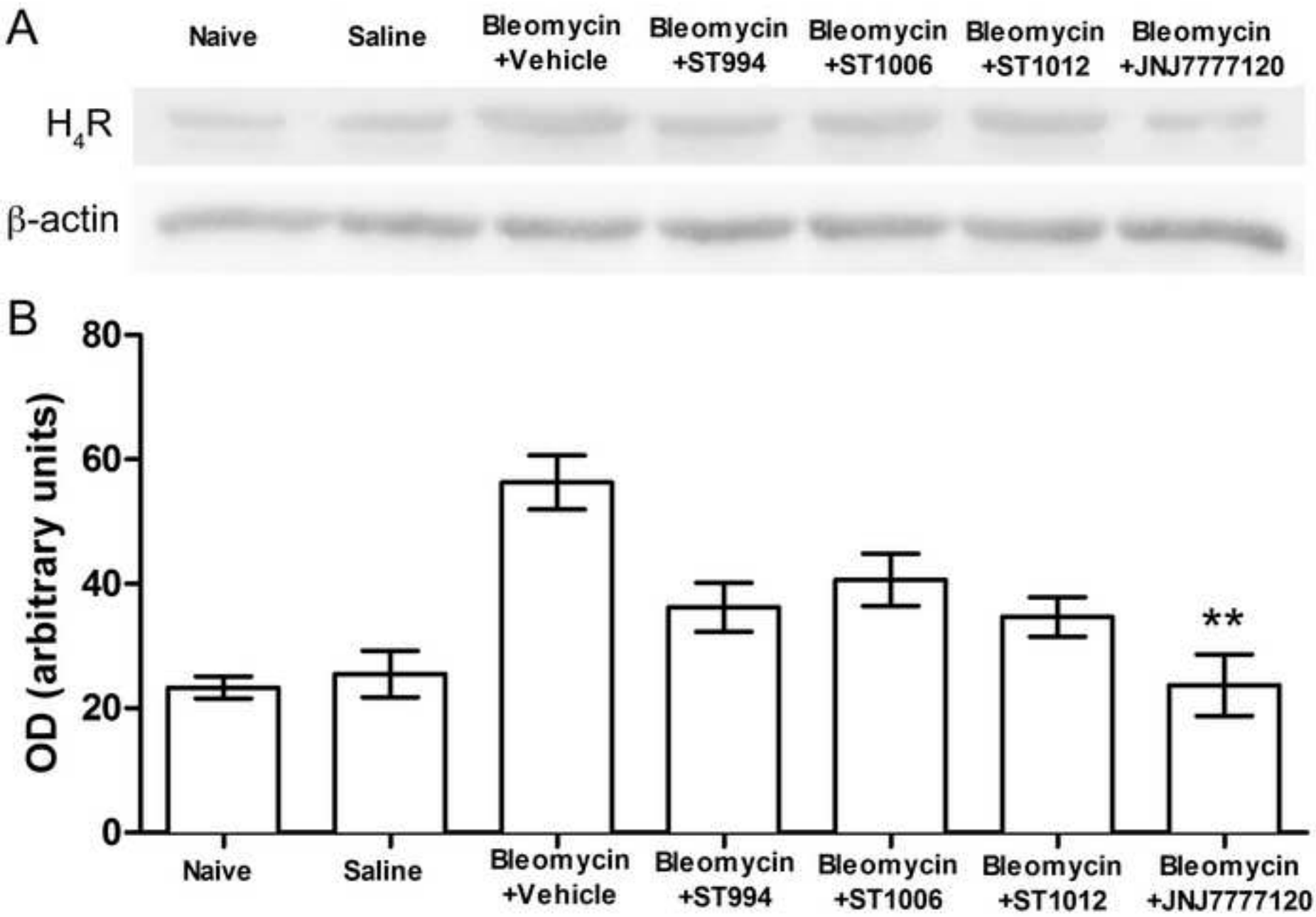

Fig. 3

Click here to download high resolution image

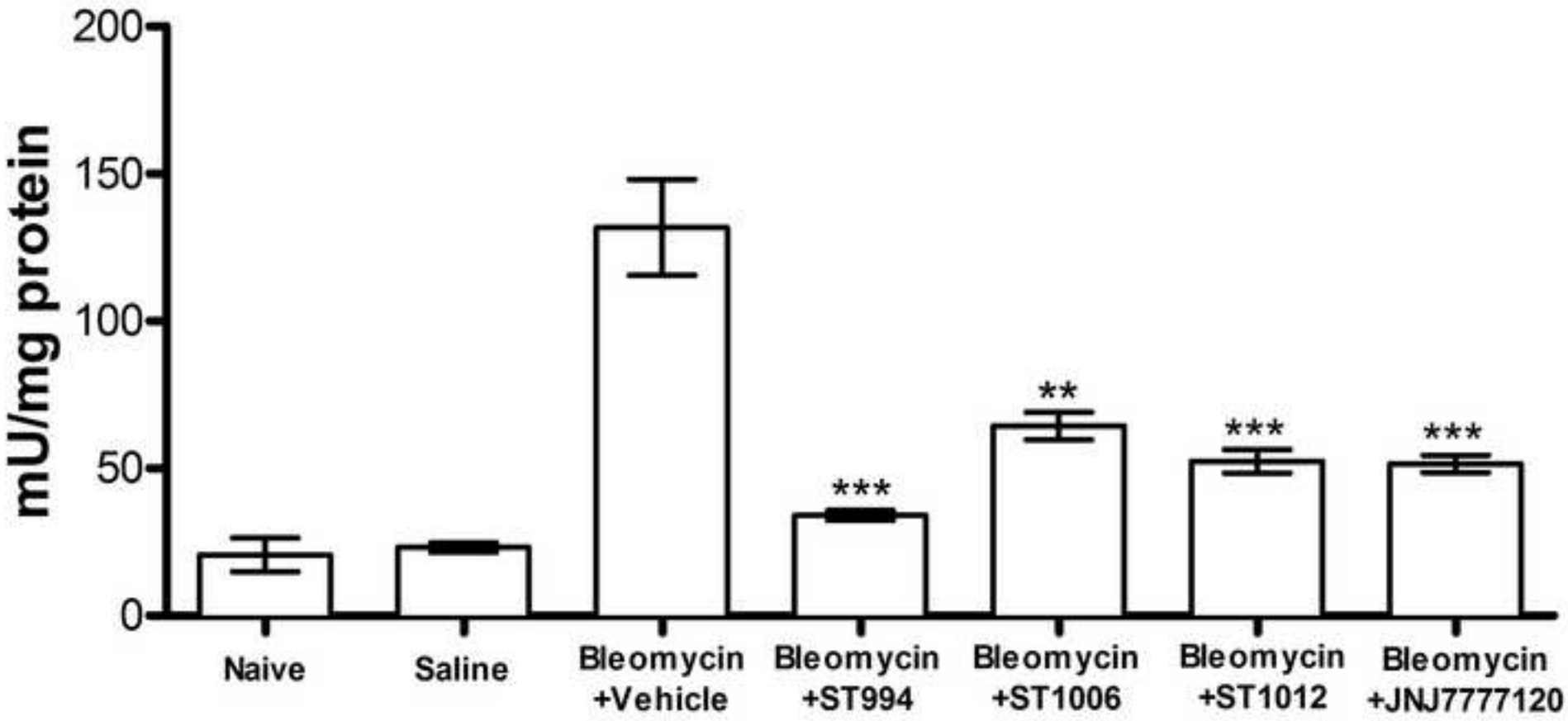

Fig. 4

Click here to download high resolution image

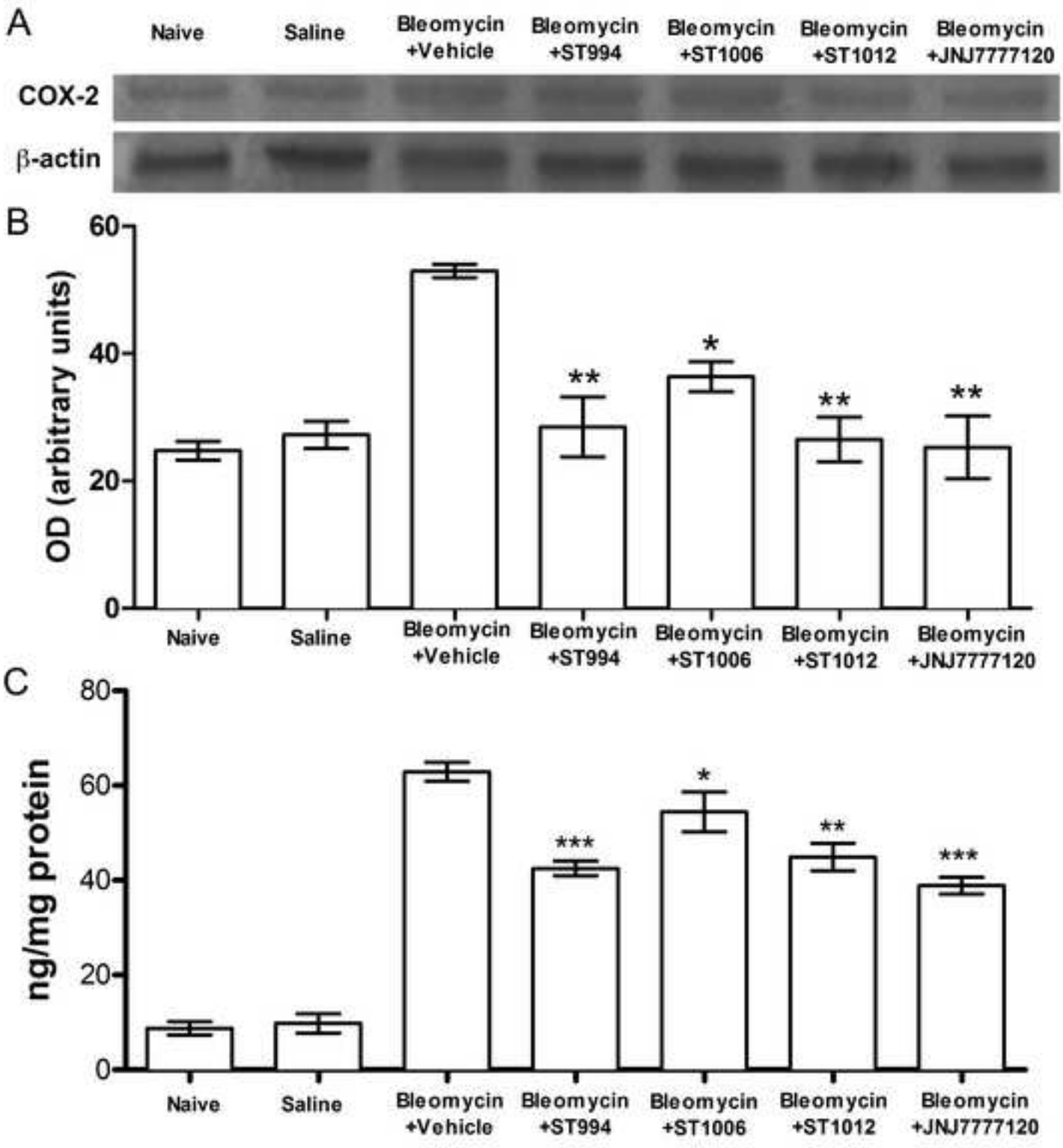

Fig. 5

Click here to download high resolution image

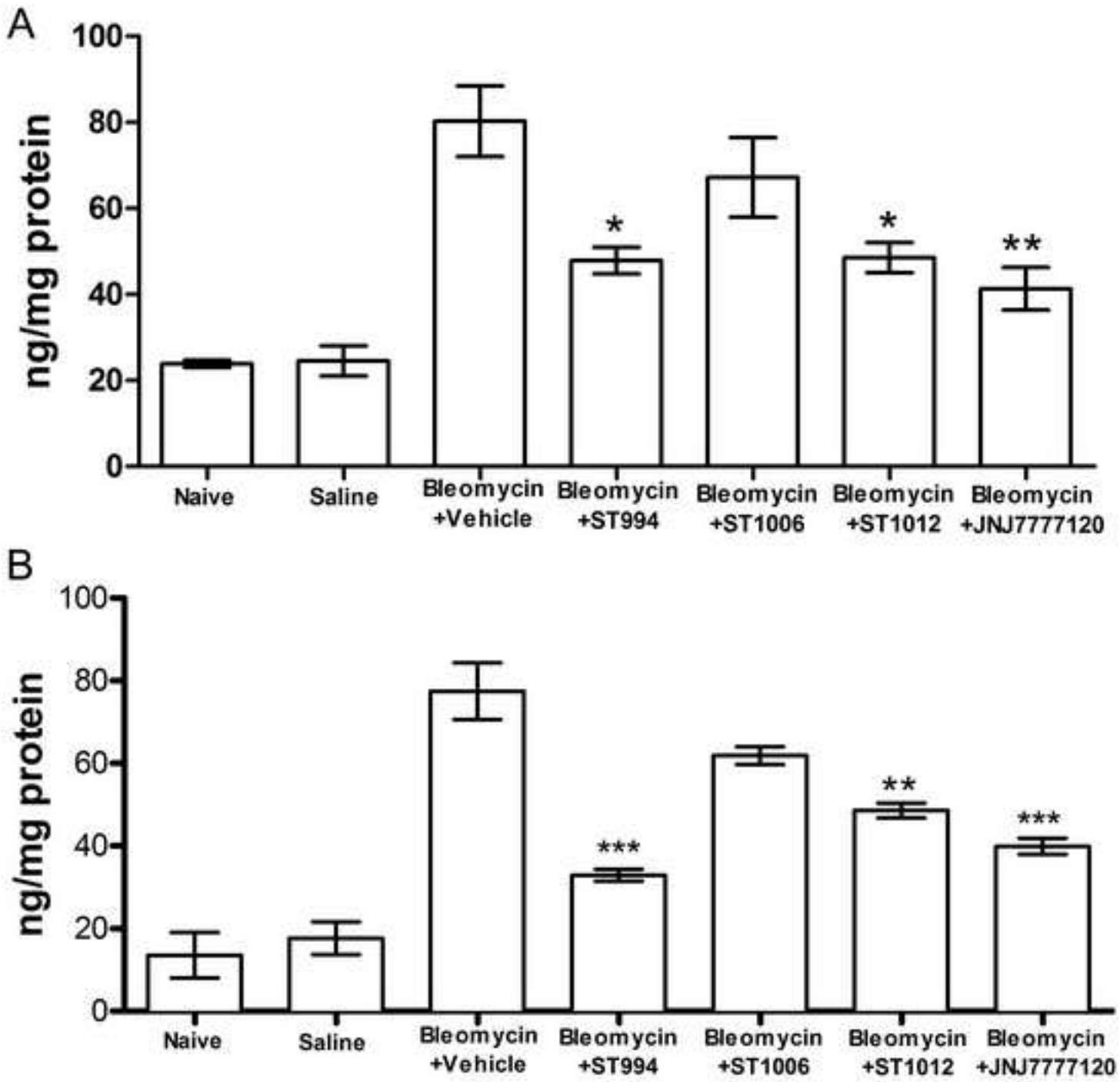

Fig. 6

Click here to download high resolution image

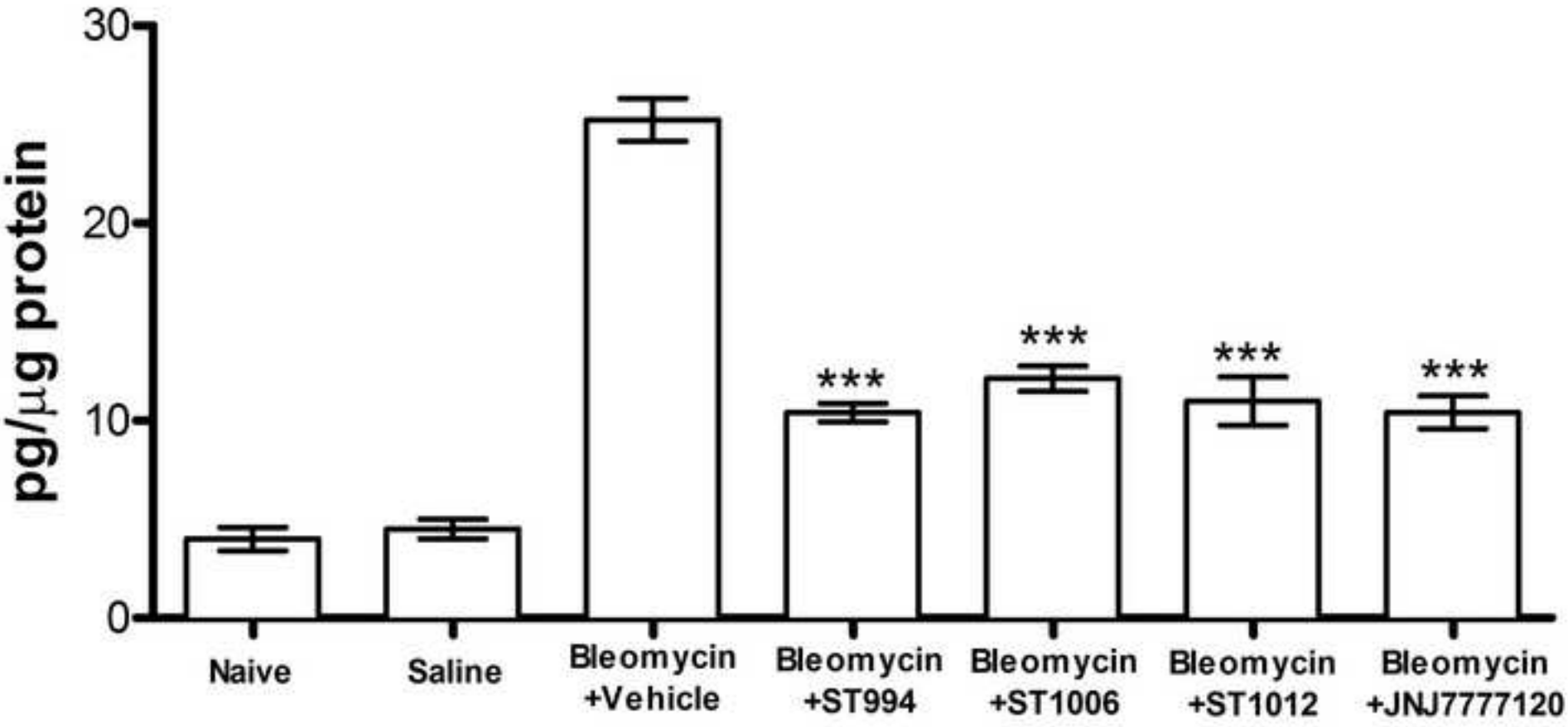

Fig. 7

Click here to download high resolution image

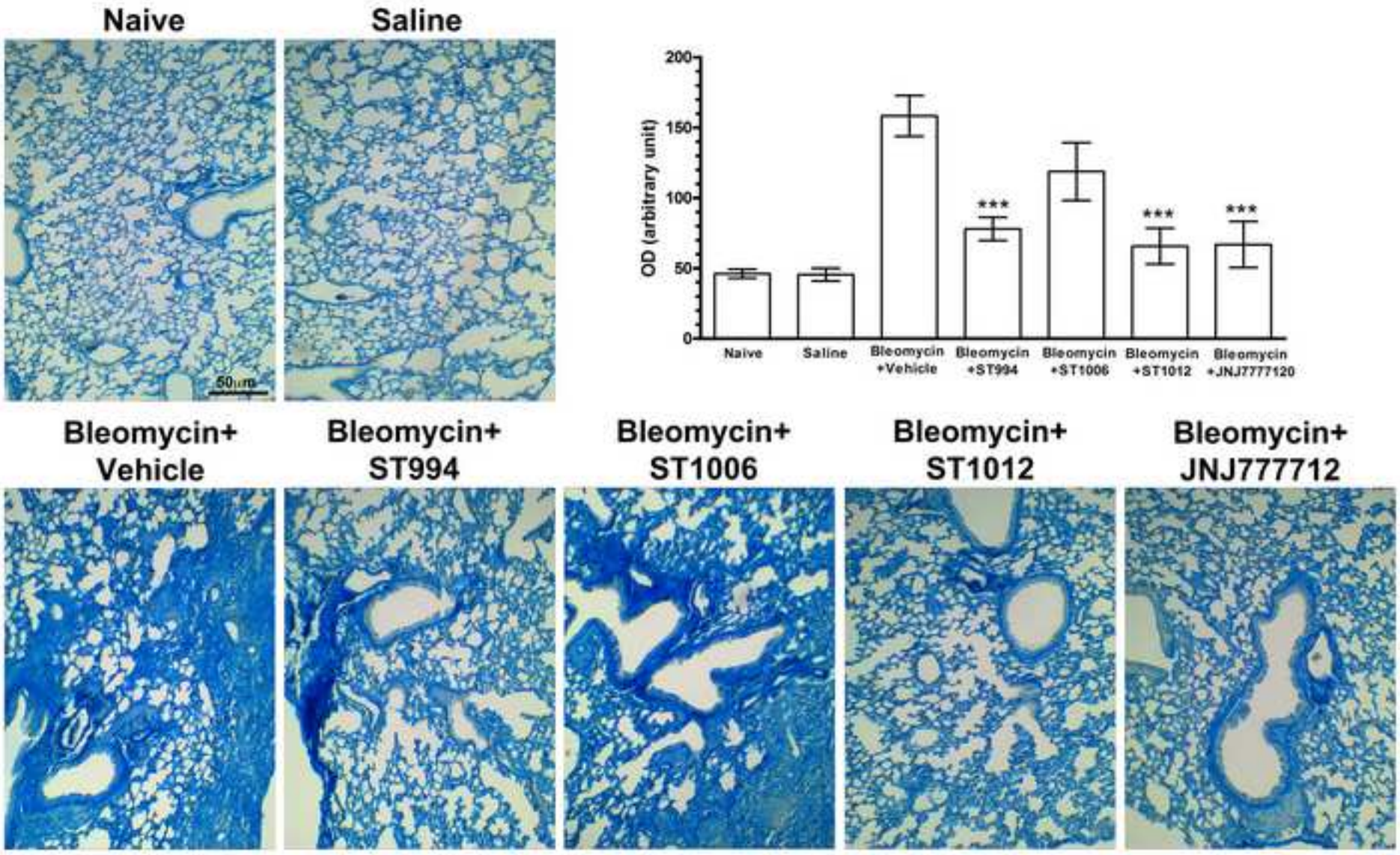

Fig. 8

Click here to download high resolution image

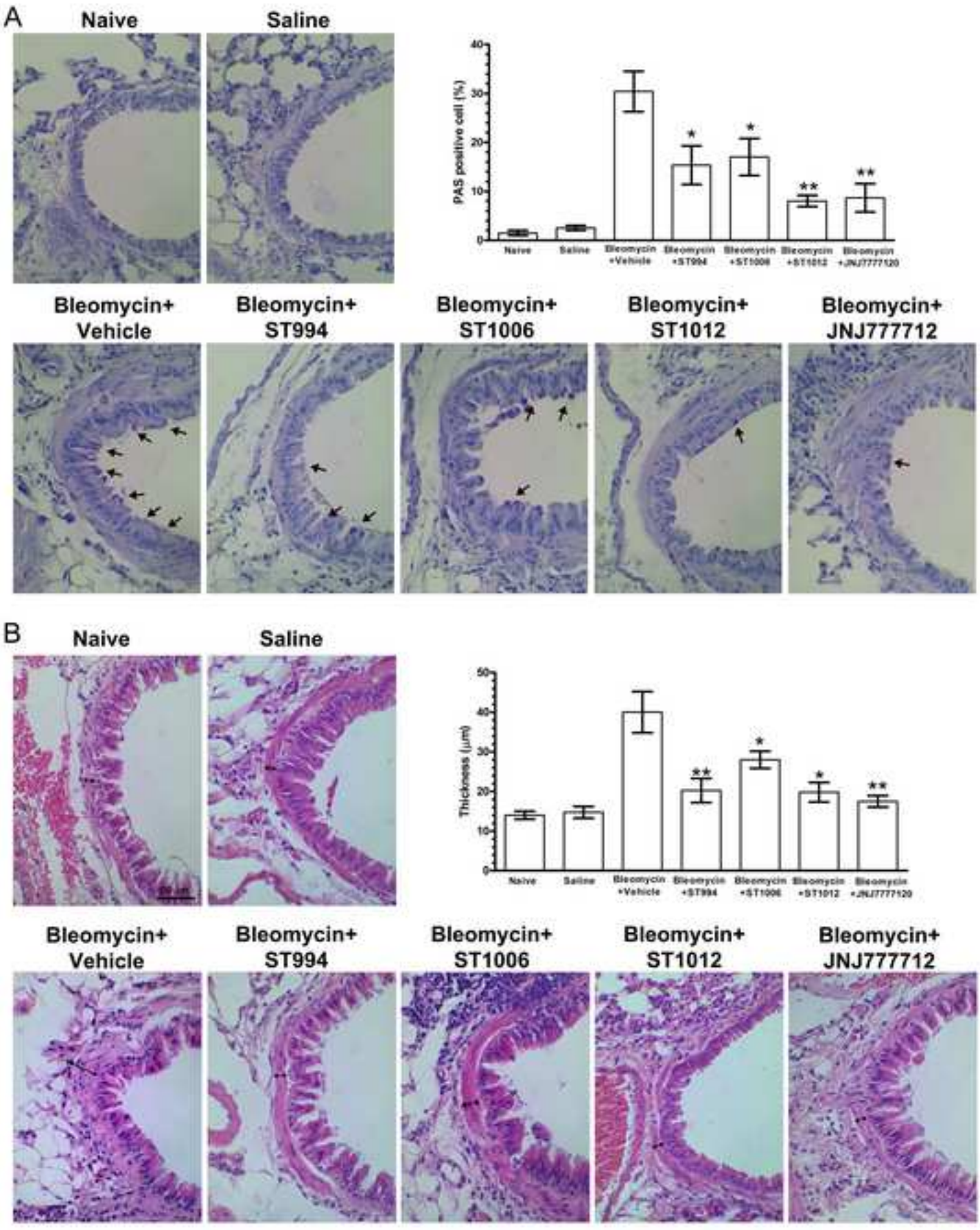

*Graphical Abstract

Click here to download high resolution image

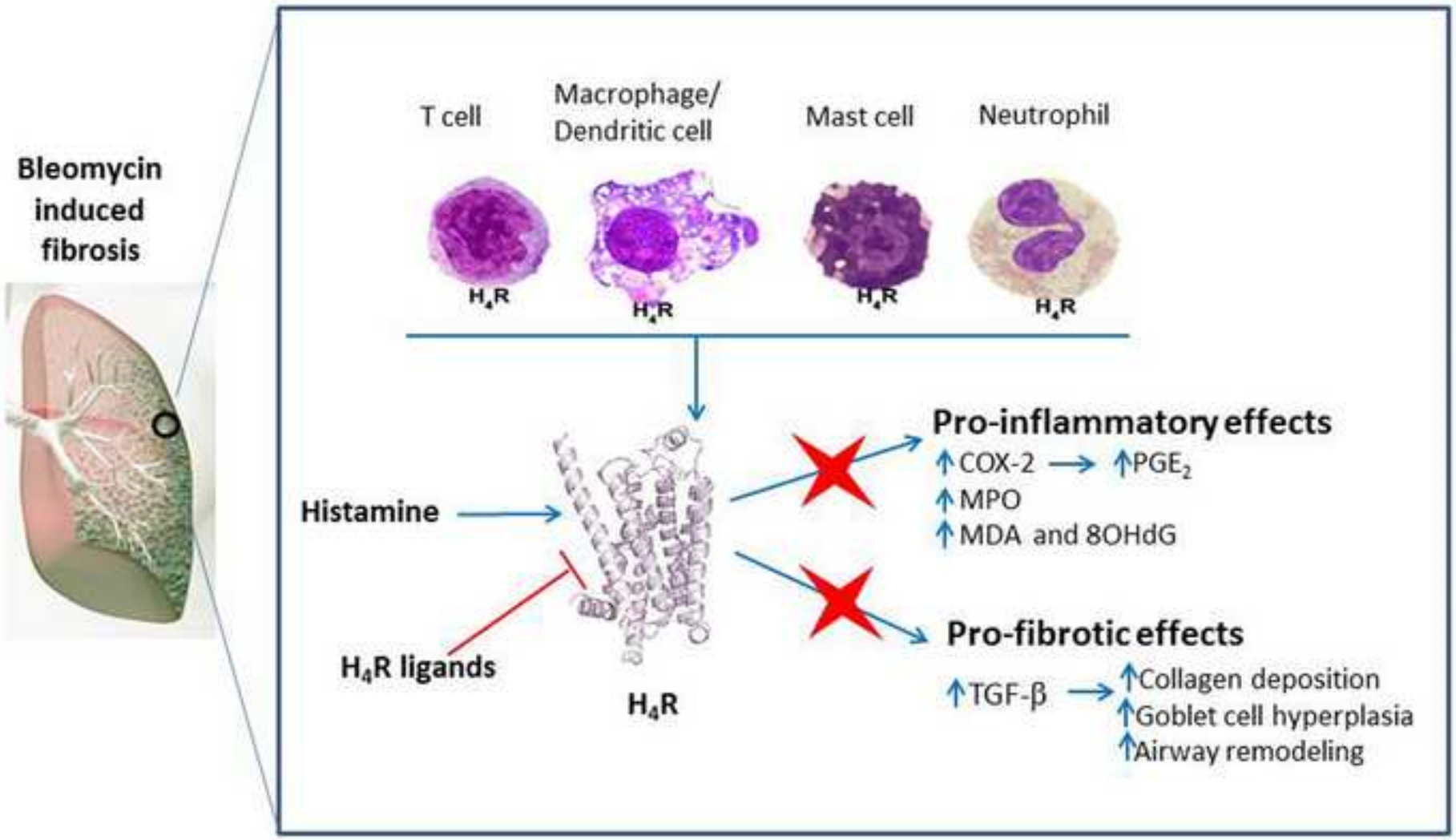

***Supplementary Figure 1**

Click here to download high resolution image

*Supplementary Figure 2

Click here to download high resolution image

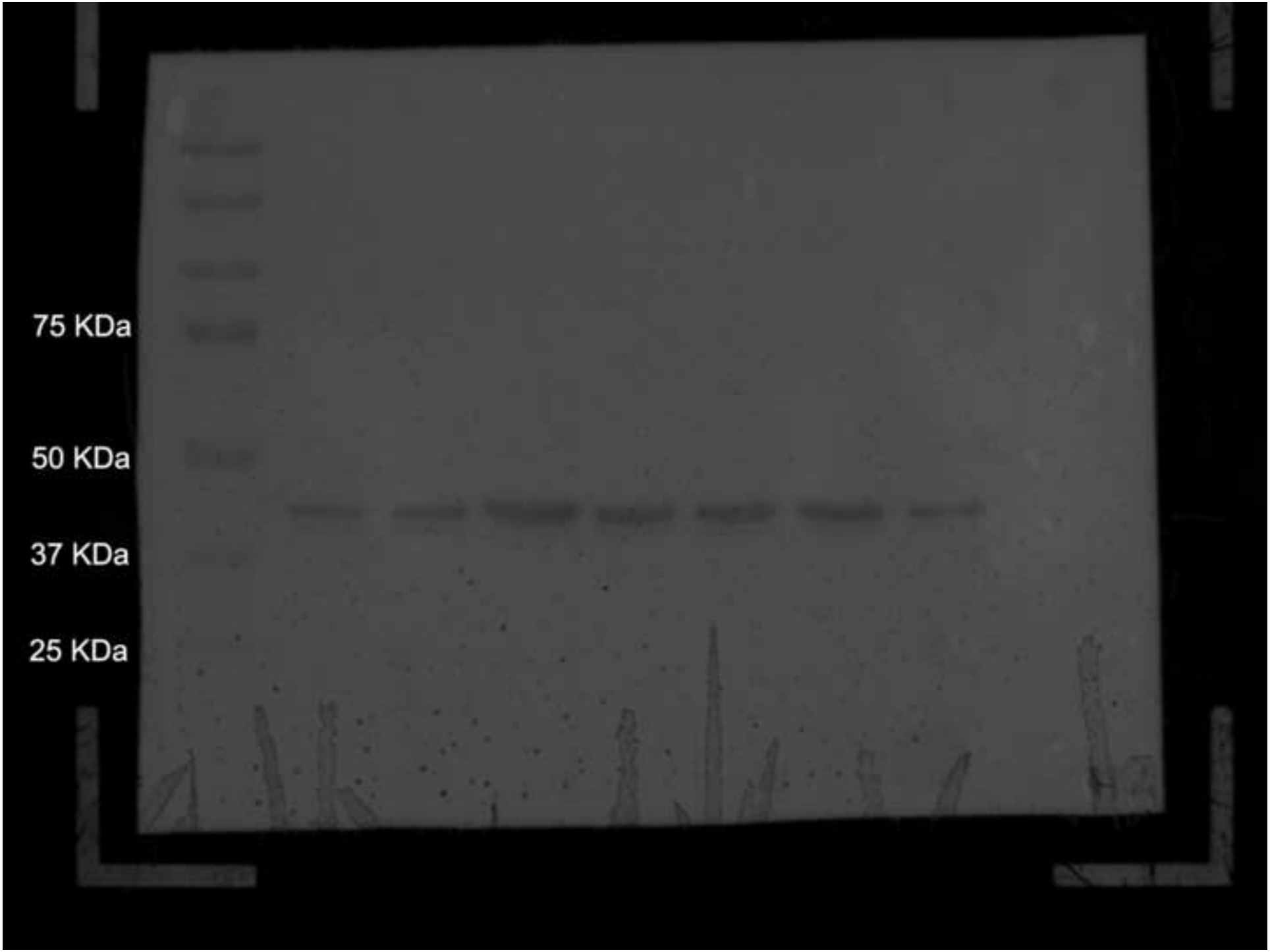

***Supplementary Figure 3**

Click here to download high resolution image

*Supplementary Figure 4

Click here to download high resolution image

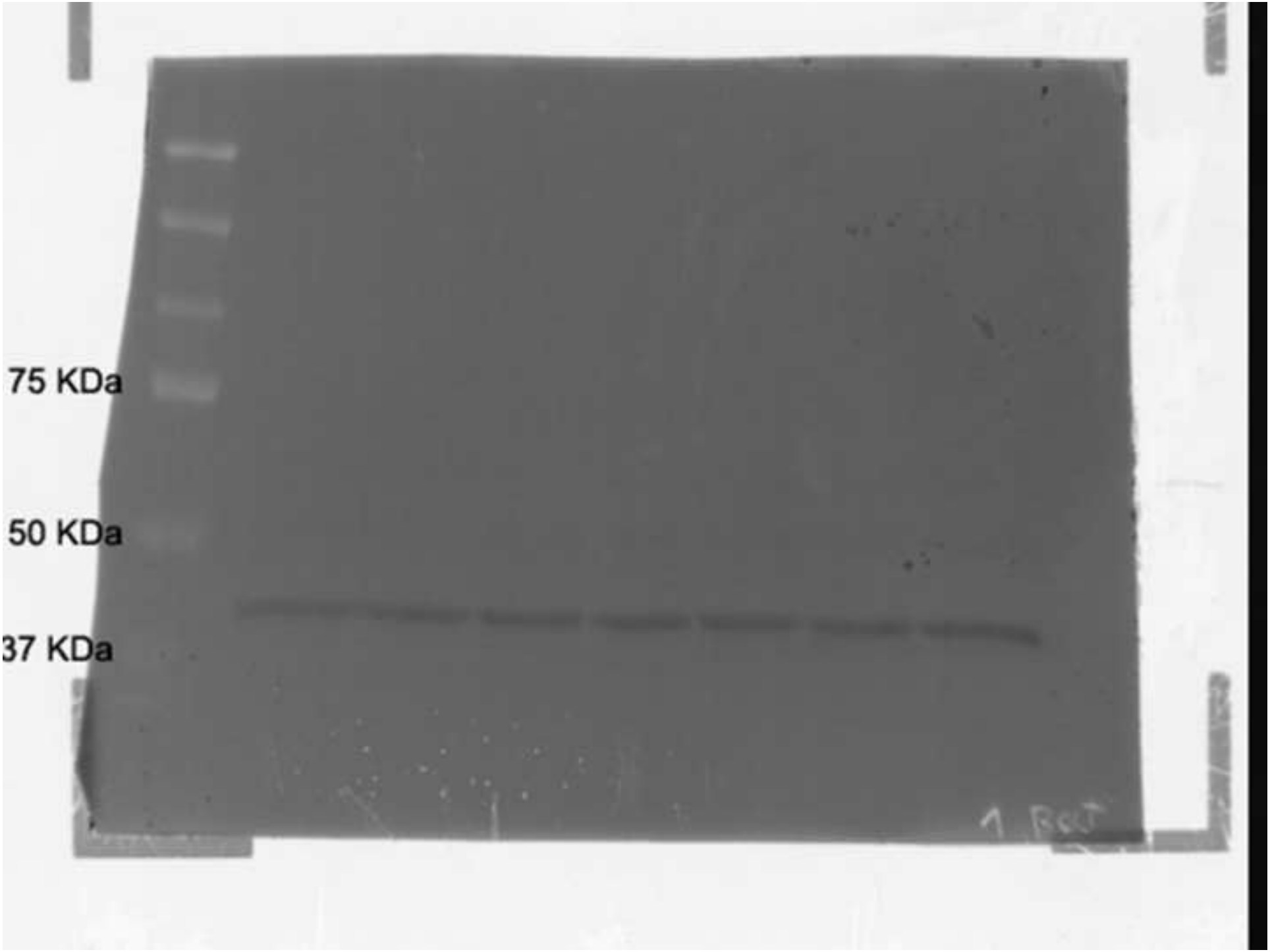

*Supplementary Figure 5

Click here to download high resolution image

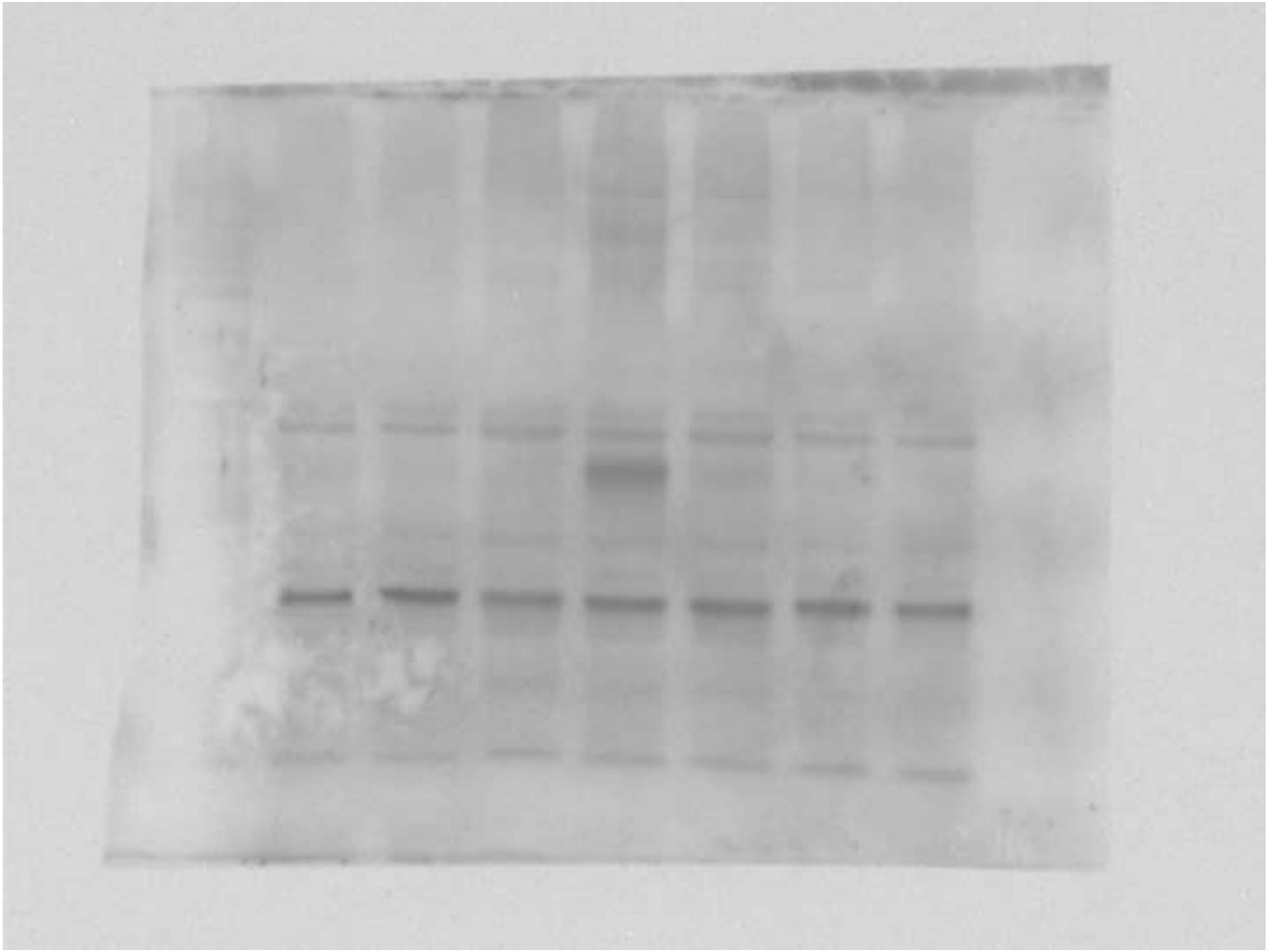

*Supplementary Figure 6

Click here to download high resolution image

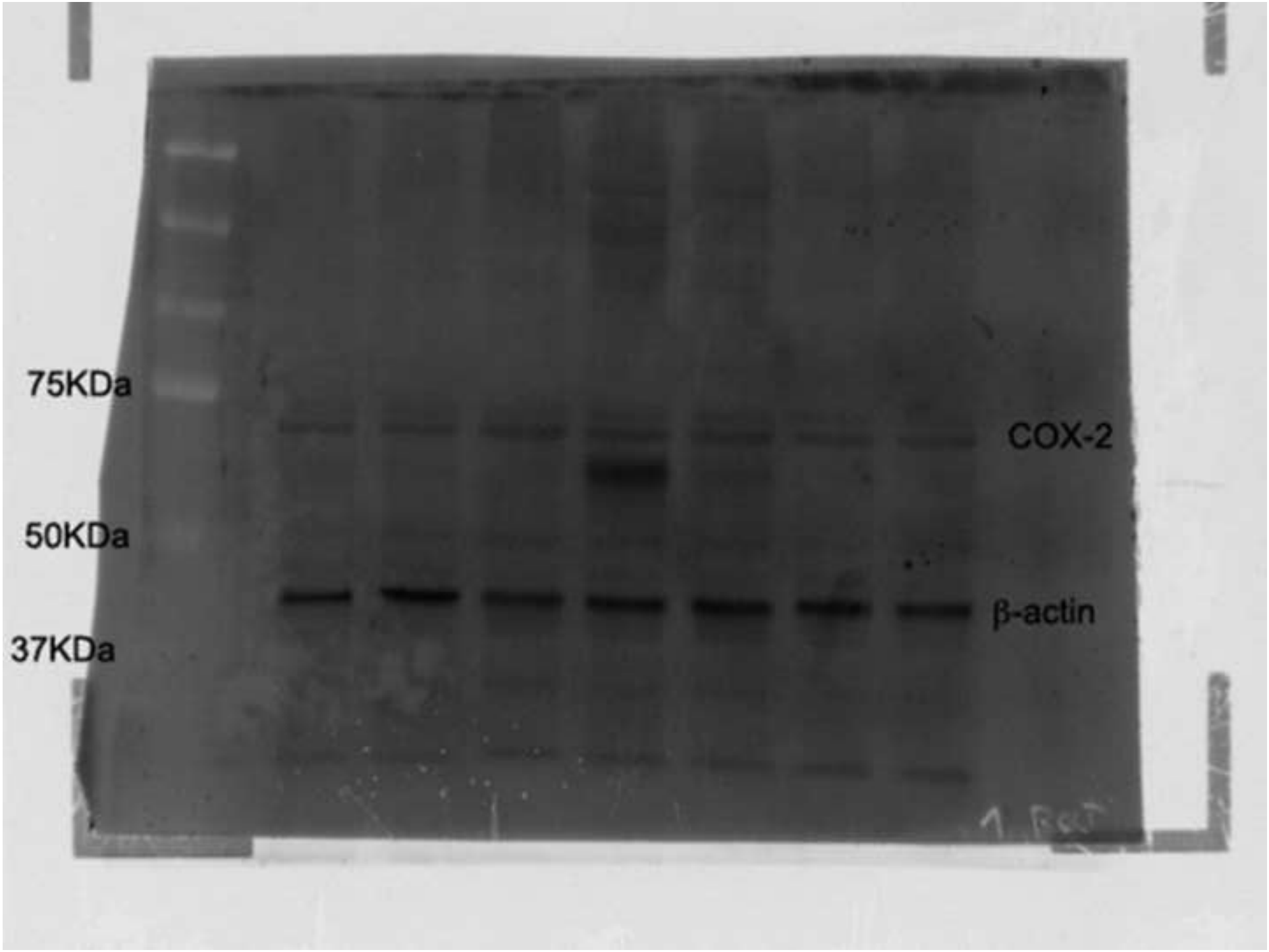

*Conflict Of Interest

Conflicts of Interest Statement

Manuscript title:

Role of Histamine H4 receptor ligands in Bleomycin-induced pulmonary fibrosis

The authors whose names are listed immediately below certify that they have NO affiliations with or involvement in any organization or entity with any financial interest (such as honoraria; educational grants; participation in speakers' bureaus; membership, employment, consultancies, stock ownership, or other equity interest; and expert testimony or patent-licensing arrangements), or non-financial interest (such as personal or professional relationships, affiliations, knowledge or beliefs) in the subject matter or materials discussed in this manuscript.

Author names:

Laura Lucarini, Alessandro Pini, Arianna Carolina Rosa,
Cecila Lanzi, Mariaconcetta Durante, Paul L Chazot, Stephane Krief,
Annemarie Schreeb, Holger Stark, Emanuela Masini

The authors whose names are listed immediately below report the following details of affiliation or involvement in an organization or entity with a financial or non-financial interest in the subject matter or materials discussed in this manuscript. Please specify the nature of the conflict on a separate sheet of paper if the space below is inadequate.

Author names:

This statement is signed by all the authors to indicate agreement that the above information is true and correct (*a photocopy of this form may be used if there are more than 10 authors*):

Author's name (typed)	Author's signature	Date
Laura Lucarini	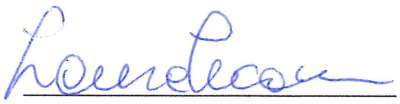	27-05-16
Alessandro Pini	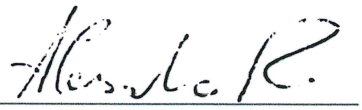	27-05-16
Arianna Carolina Rosa	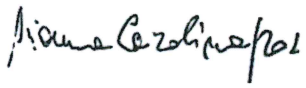	27-05-16
Cecila Lanzi		27-05-16
Mariaconcetta Durante	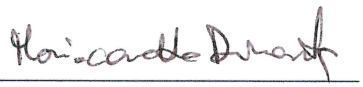	27-05-16
Paul L Chazot	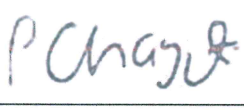	27-05-16
Stephane Krief	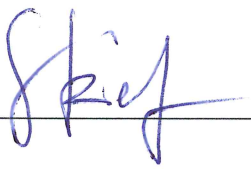	27-05-16
Annemarie Schreeb	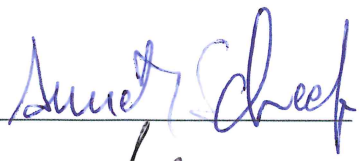	27-05-16
Holger Stark	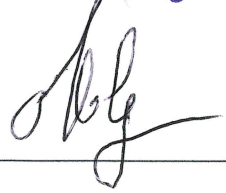	27-05-16
Emanuela Masini		27-05-16